PAPER

Check for updates

Sumanene-based triazole-linked receptors

Joachim Ażgin,[a] Stanisław Kulczyk, [ID][a] Hidehiro Sakurai, [ID][bc]
Wojciech Wróblewski*[a] and Artur Kasprzak [ID] *[a]

Designing molecular receptors featuring the bowl-shaped sumanene motif for detecting metal cations constitutes an emerging field of applied supramolecular chemistry of this buckybowl. In this work, we successfully synthesized a new class of sumanene-based receptors, whose key structural feature was the presence of two or three sumanene units linked via 1,2,3-triazole skeletons generated in a 1,3-dipolar cycloaddition reaction (click chemistry approach). It was found that the designed compounds detect metal cations in solution (spectrofluorometric studies), as well as in heterogeneous systems (polymeric membranes of potentiometric sensors). In terms of optical studies in solution, the title molecules exhibited fluorescence quenching behaviours upon addition of metal cations, with Stern–Volmer constant values at the level of 10^6 M^{-1}. The spectrofluorometric and potentiometric results were in good agreement, revealing the preferential binding of lithium (Li^+), caesium (Cs^+), or copper(II) (Cu^{2+}) cations, depending on the receptor structure. Density functional theory (DFT) computational studies were also performed on the structure and receptor properties of the title molecules. The results indicate attractive possibilities for the design of novel organic materials based on the sumanene scaffold and the ability to tune the properties of sumanene-based receptors for recognition of different metal cations.

Sumanene (**1**, Fig. 1) is a bowl-shaped and π-conjugated fragment of fullerene C_{60}, and the supramolecular chemistry of sumanene has developed remarkably in the last several years.[1–5] The most representative examples include the design of functional materials dedicated to dielectric devices,[6–8] metal–organic frameworks and organized molecules,[9,10] or molecular receptors.[11–13] The last application area might be considered as a natural evolution within sumanene science over the years, which began from numerous computational studies on the cation–π interactions between sumanene and metal cations,[14–17] as well as demonstrated possibilities of the formation of sumanene organometallic complexes.[18–21]

In terms of sumanene-based molecular receptor science, recent reports revealed the possibility of the selective detection of caesium (Cs^+) cations by means of site-selective cation–π interactions with the inclusion of concave sites of sumanene bowls (formation of sandwich complexes). From a structural viewpoint, these studies employed receptors based on mono-,[11,13,22,23] tris-,[12,22,24–27] or tetra[27,28] substituted sumanene
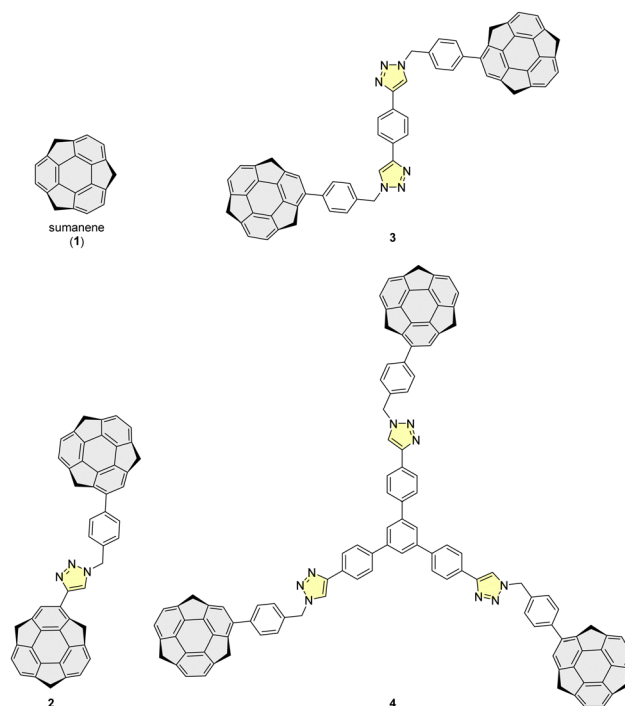
[a] Faculty of Chemistry, Warsaw University of Technology, Noakowskiego Str. 3, 00-664 Warsaw, Poland. E-mail: artur.kasprzak@pw.edu.pl, wojciech.wroblewski@pw.edu.pl

[b] Division of Applied Chemistry, Graduate School of Engineering, The University of Osaka, 2-1 Yamadaoka, Suita, 565-0871 Osaka, Japan

[c] Innovative Catalysis Science Division, Institute for Open and Transdisciplinary Research Initiatives (ICS-OTRI), The University of Osaka, Suita, Osaka 565-0871, Japan

Fig. 1 Structures of sumanene (**1**) and target compounds **2–4** (sumanene skeleton – grey; 1,2,3-triazole skeleton – yellow).

derivatives functionalized with various moieties, mostly aromatic skeletons.

The molecular recognition process can be spectroscopically and electrochemically tracked using voltammetric[11,13,24,28] and potentiometric[22,26] methods. The potentiometric method is considered especially attractive because, in contrast to voltammetric sensors, potentiometric techniques do not require the presence of a redox-active moiety in the receptor molecule, and this potentially expands the scope of derivatives that can be used as ionophores. Previous studies demonstrated that sumanene derivatives might serve as ionophores in potentiometric sensors, featuring good selectivity toward Cs^+ with a satisfactory limit of detection (LOD) value at the micromolar concentration level.

Copper-catalysed azide–alkyne cycloaddition (CuAAC) is an efficient *click chemistry* reaction that can be applied, among others, to the synthesis of complex receptor molecules consisting of a recognition unit and a reporter probe that are coupled.[29] As a result of a click reaction, 1,4-disubstituted 1,2,3-triazole products are formed, where the 1,2,3-triazole ring often plays the role of a simple covalent linker of macromolecular structures.[30] However, the 1,2,3-triazole skeleton can also be employed as a building block for the design of functional receptors.[31] These specific binding properties result from the presence of nitrogen atoms with lone electron pairs, providing binding sites to coordinate transition metal cations, as well as C–H hydrogen bond donors in the heteroaromatic system, and enabling CH···anion hydrogen bonding interactions.[31,32] Therefore, 1,2,3-triazole-based compounds have widely been reported as highly effective chromogenic or fluorogenic receptors for cations, anions, and neutral molecule-sensing.[33,34]

Potentiometric cation and anion detection was attempted using 1,2,3-triazole-based ionophores introduced into polymeric membranes of ion-selective electrodes (*e.g.*, tetratriazole-linked calix[4]arene[35] or triazolophane derivatives[36] displaying high selectivity for Cu^{2+} cations or halide anions, respectively). However, the introduction of the ferrocene unit (*via* click reaction) into the receptor structure led to the development of voltammetric sensors, where the redox properties of ferrocene were affected by cation or anion binding to the triazole moiety.[33,37,38]

Herein, we report the synthesis of bis- and tris-sumanenes (compounds 2–4, Fig. 1), as well as spectrofluorimetric and potentiometric studies on their receptor properties with the goal of the detection of selected metal cations. The binding mode of the designed receptors relies on cation–π interactions with the inclusion of sumanene skeletons, as well as N-donor binding sites of 1,2,3-triazole moieties. From the synthetic viewpoint, we selected a *click chemistry* (1,3-dipolar cycloaddition) approach for the design of target receptors, not only taking into account the versatility of this methodology in the generation of various applied materials but also considering the prospectively attractive receptor properties of 1,2,3-triazoles in conjunction with the sumanene motif, as noted above.

Inspired by a report[39] on the unexpected Li^+-detection property of sumanene-based bis(terpyridine)-ruthenium(II)

complexes, among which several molecules were based on two linked sumanene skeletons, we anticipated tuned receptor properties of compounds 2–4 in comparison to known Cs^+ receptors composed of one sumanene skeleton in the formula. According to our studies reported in this work, bis- and tris-sumanenes exhibit tuned selectivity toward Cs^+, Li^+, or Cu^{2+}. This not only reveals a structure–receptor property relationship but also represents a step forward in expanding the scope of possible analytes detected by carefully designed sumanene-based receptors. Our studies also demonstrated that the location of the 1,2,3-triazole unit in the designed receptors (direct attachment to the sumanene skeleton or *via* a linker) is crucial in terms of the selectivity of the receptor, which is an important outcome for further studies in the discussed area.

Results and discussion

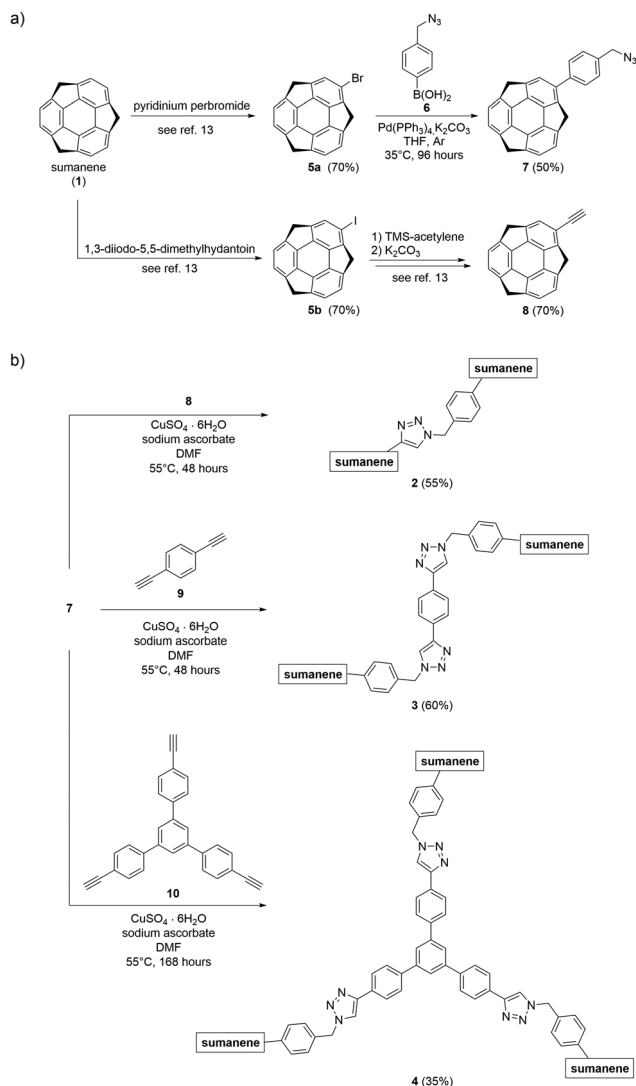### Synthesis and photophysical characterization of compounds 2–4

Full experimental details on the synthesis are presented in the SI, Section S1. Scheme 1 shows the synthesis paths towards 2–4. The starting material for the synthesis of compounds 2–4, namely a sumanene derivative bearing an azide moiety (compound 7), was synthesized (60%) by means of Suzuki–Miyaura cross-coupling between 2-bromosumanene (5a)[40] and (4-(azidomethyl)phenyl)boronic acid (6).[41]

Optimization experiments revealed that the highest reaction yield was observed for the reaction conducted at 35 °C for 96 h under an argon atmosphere and in the presence of tetrakis-(triphenylphosphine)palladium(0) as the catalyst. Synthesis paths towards 2–4 were based on the similar conditions of a 1,3-dipolar cycloaddition reaction (*click chemistry* approach) using starting material 7 in each case and employing copper(II) sulphate pentahydrate with sodium ascorbate as the catalytic mixture, in *N,N*-dimethylformamide (DMF) as the solvent, and at 55 °C. 2-Ethynylsumanene (8),[40] 1,4-diethynylbenzene (9), or 1,3,5-tris(4-ethynylphenyl)benzene (10)[42] were subjected to reaction to obtain compound 2, 3, or 4, respectively.

During optimization experiments for the production of compounds 3–4, we were able to identify the formation of side products comprising unreacted ethynyl moieties (compounds of mono- or di-substitution; see the details on optimization experiments in the SI, Section S1). The highest isolated yields for compounds 2–3 (55–60%) and 4 (35%) were observed when the reaction was conducted for 48 h and 168 h, respectively. Longer reaction times did not provide higher yields of target products. Interestingly, we observed that the highest yield for the transformation of 7 to *click chemistry*-derived 2–4 was achieved when starting material 7 was subjected to the reaction just after its preparation, suggesting that longer storage times for compound 7 (even when storing the sample under an argon atmosphere at −28 °C) were not beneficial.

1D and 2D NMR spectroscopy, as well as HRMS spectrometry supported the formation of pure compounds 2–4 and 7 (refer to the SI, Sections S1–S3, for the compound

Scheme 1 Synthesis of starting materials 7–8 (a) and compounds 2–4 (b).

Fig. 2 Selected insets of the ^{1}H NMR spectra (600 MHz, DMSO-d_6) of compounds 2–4. Graphical representations of the structural moieties ascribed to given groups of signals are also presented. Selected peaks are marked for image clarity. The same colour does not correspond to the same chemical shift in the NMR spectrum.

which was ascribed to a different sumanene skeleton substitution in 2 (two sumanene bowls featured different substituents at the aromatic position) in comparison to 3–4 (two sumanene bowls featured the same substituent at the aromatic position).

Additionally, ^{1}H DOSY NMR experiments revealed that the signals observed in the NMR spectra of 2–4 originated from one molecule, which further supported the sample composition. The hydrodynamic radius $(r_{\text{solv,H}})^{43}$ for compound 4 (approximately 1.3 nm) was found to be higher than the hydrodynamic radii of 2 (approximately 0.8 nm) and 3 (approximately 0.5 nm). Finally, HRMS spectral analyses revealed that the experimental and computed isotopic patterns for 2–4 and 7 were in good agreement, ultimately confirming the successful isolation of target sumanene derivatives.

Fig. 3 shows a summary of the UV-vis and fluorescence spectra of compounds 2–4 (in THF; see the 3D fluorescence spectra of 2–4 in Section S4, SI). The UV-vis spectra of compounds 2–4 feature absorption maxima (λ_{max}) located in

characterization data). Fig. 2 presents a comparison of the ^{1}H NMR spectra of 2–4 (in DMSO-d_6). For the NMR spectra of compounds 2–4, the most diagnostic changes compared to the spectra of the starting materials (7–10) were the disappearance of signals coming from the ethynyl moieties (from starting materials 8–10), along with the appearance of characteristic ^{1}H NMR signals of 1,2,3-triazole moieties (δ_H between 8.82 and 8.73 ppm).

Additionally, the ^{1}H and $\{^1\text{H}\}^{13}$C NMR spectra of compounds 2–4 not only featured signals coming from the aromatic moieties but also characteristic ^{1}H NMR signals for sumanene H-benzylic, *endo* (δ_H between 3.62 and 3.28 ppm) and H-benzylic, *exo* (δ_H between 5.04 and 4.67 ppm) protons, as well as ^{13}C NMR signals of C-benzylic ^{13}C nuclei (δ_c between 52.8 and 41.2 ppm).

Notably, the NMR spectra of 3–4 suggested that these compounds were chemically equivalent in solution. It was also observed that the resonances for benzylic protons of 3–4 were relatively similar to each other and different than those for 2,
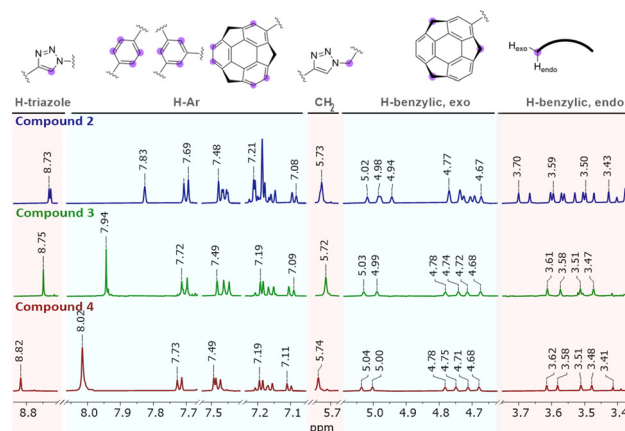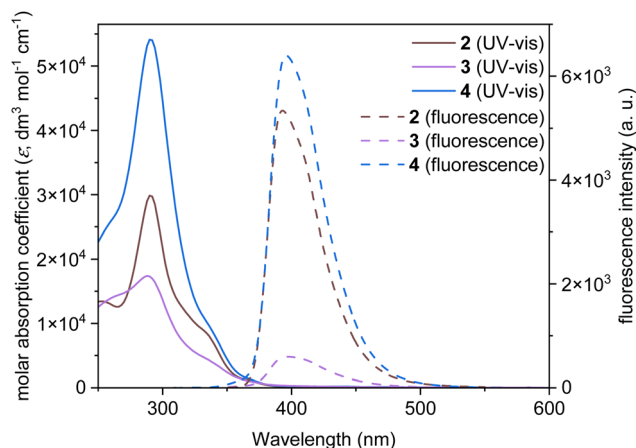

Fig. 3 UV-vis (THF) and fluorescence spectra (THF, $\lambda_{\text{ex,2}}$ = 290 nm, $\lambda_{\text{ex,3}}$ = 288 nm, $\lambda_{\text{ex,4}}$ = 290 nm) of compounds 2–4 (C = 2 × 10^{-5} M).

the range 250–375 nm, with molar absorption coefficient (ε) values ranging from 1.5×10^4 to 5.5×10^4 dm^3 mol^{-1} cm^{-1}. The fluorescence spectra of compounds **2–4** show one emission maximum (λ_{em}) located at approximately 400 nm. The highest ε and fluorescence intensity values were found for compound **4**, whereas the lowest were for compound **3**. Density functional theory (DFT) and time-dependent DFT (TD-DFT) computations[44–48] (B3LYP[49]/3-21G[50]) for compounds **2–4** revealed good accordance between observed and calculated transitions in the UV-vis spectra (refer to the SI, Section S7, for the data). Additionally, the HOMO–LUMO energy gaps for compounds **2–4** were very similar (4.42–4.43 eV), which is consistent with the observed lack of significant differences in their experimental fluorescence spectra (λ_{em} between 394–397 nm).

Receptor properties of compounds 2–4

Supramolecular interactions between bis- and tris-sumanenes **2–4** and selected metal cations were investigated in solution using fluorescence spectroscopy. Due to the limited solubility of the sumanene derivatives in water, the experiments were carried out in a 1:1 mixture of THF and water (see the full experimental details for the spectrofluorimetric titrations in Section S1.4, SI).

Fig. 4 presents the results of fluorescence spectra titration curves of receptors **2–4** with various metal cations (Li$^+$, Cs$^+$, and Cu^{2+} were included in the comparison, taking into account previous reports on Li$^+$- and Cs$^+$-oriented sumanene receptors, and the presence of 1,2,3-triazole moieties in **2–4** structures, regarding Cu^{2+}). The addition of increasing molar equivalents of metal cations caused a systematic decrease in the fluorescence intensity (λ_{em} = 400 nm); however, the extent of signal quenching varied depending on the specific cations and the receptor studied.

The presence of Li$^+$ cations resulted in the fluorescence quenching of all tested receptors, which was ascribed to the dynamic formation of cation–π systems. However, high selectivity of Li$^+$ complex formation was noted only for receptor **2**, whereas derivatives **3** and **4** exhibited comparable affinity for Cu^{2+} and Cs$^+$ cations, respectively. Moreover, the most significant changes in intensity of the fluorescence signal upon addition of Li$^+$ and Cs$^+$ cations were noted for tris-sumanene receptor **4** (see Fig. S37 and S38, SI, presenting the emission spectra of **4** during titrations with Li$^+$ and Cs$^+$ cations). It should also be emphasized that similar turn-off fluorescence behaviour was observed during our previous studies on sumanene-based Cs$^+$ cation receptors.[22]

Stern–Volmer constants were determined using non-linear curve fitting of fluorescence titration data to the modified Stern–Volmer eqn (1). This equation describes fluorescence quenching in a system, in which only a fraction of the fluorophore is accessible to the quencher (*e.g.*, due to partial aggregation of the receptor molecules in solution).[51–53] The calculated Stern–Volmer constants (K_{SV}) reflect the strength of interactions between metal cations and receptors **2–4** observed during spectrofluorimetric experiments. They were collected
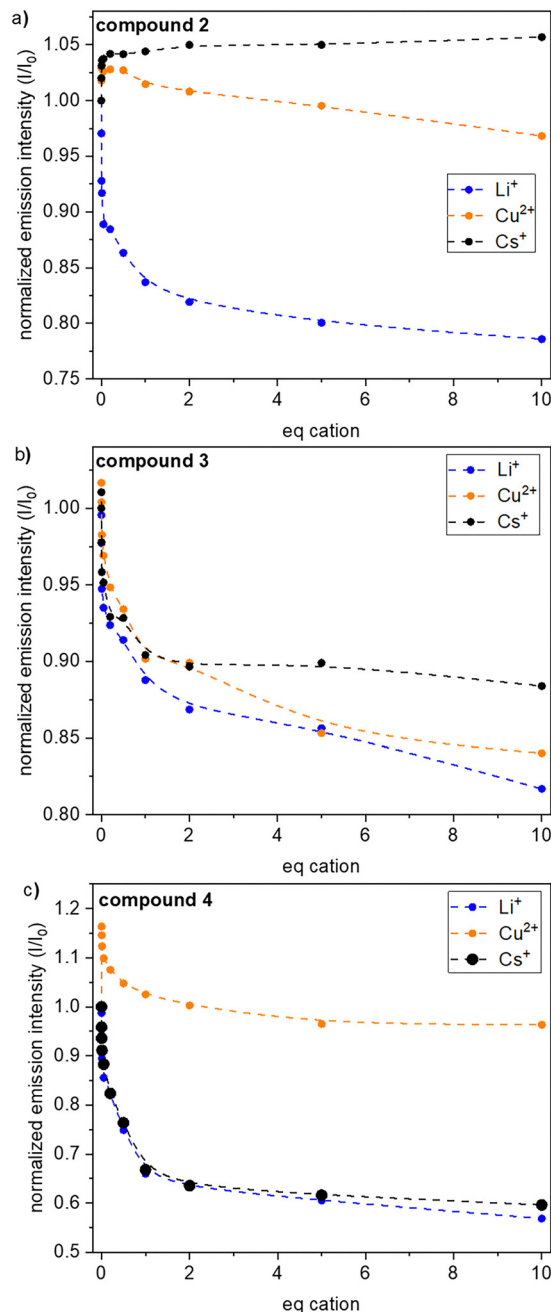

Fig. 4 Fluorescence spectra titration curves for receptors **2** (a), **3** (b) and **4** (c) with Li$^+$, Cs$^+$, and Cu^{2+} cations (THF:water = 1:1 v/v, C = 0.02 mM).

Table 1 Values of Stern–Volmer constants determined for derivatives **2–4** using a non-linear curve fitting of the fluorescence titration data presented in Fig. 3

Compound	Li$^+$ K_{SV} [10^6 M^{-1}]	Cs$^+$ K_{SV} [10^6 M^{-1}]	Cu^{2+} K_{SV} [10^6 M^{-1}]
2	12.6	—	—
3	2.6	6.7	1.0
4	2.48	3.87	—

and appear in Table 1 (plots depicting non-linear curve fitting of the fluorescence titration data and fitting parameters are

presented in Section S6, SI).

$$\frac{I_0}{I_0 - I} = \frac{1}{f_a \cdot K_{SV} \cdot c} + \frac{1}{f_a} \quad (1)$$

where I_0 and I denote the fluorescence intensities of the receptor molecule in the absence and presence of quencher, respectively; c denotes quencher concentration; K_{SV} denotes the Stern–Volmer constant; and f_a denotes the fraction of the fluorophore accessible to the quencher.

The selectivity of metal cation recognition was also studied in a heterogeneous system, i.e., the bis- and tris-sumanene derivatives **2–4** were introduced into polymeric membranes based on plasticized poly(vinyl chloride) (PVC), used commonly as a membrane matrix of ion-selective electrodes. Potentiometric selectivity coefficients, reflecting the influence of a given interfering cation (Me) on the ion-selective sensitivity for the chosen primary ion, were determined in this regard. Assuming that the tested sumanene derivatives **2–4** work as neutral carriers, a lipophilic anionic additive (potassium tetrakis[3,5-bis(trifluoromethyl)phenyl]borate; KTFPB) was added to the membranes to achieve their permselectivity and provide proper operation of the sensors.[54–56]

The ion selectivity of the polymeric membranes containing studied receptors **2–4** is graphically presented in Fig. 5 and collected in Table 2 (the values of the selectivity coefficients were calculated for Na$^+$ as an arbitrarily chosen primary ion). It should be noted that the presence of anionic sites (TFPB$^-$) induces enhanced membrane selectivity for lipophilic cations (e.g., Cs$^+$), which is characterized by less negative values of the standard molar Gibbs free energy of hydration.[57] Therefore, reliable evaluation of the results requires the selectivity of the polymeric layers doped with receptors **2–4** to be compared with the same values determined for blank membranes, containing only KTFPB.

Table 2 Values of the selectivity coefficients ($\log K_{Na,Me}$) of potentiometric sensors formulated with receptors **2–4** and **11** (10 mol% KTFPB) and without a receptor (blank membrane) in PVC/o-NPOE membranes (mean values were calculated for 3 electrode specimens)

	$\log K_{Na,Li}$	$\log K_{Na,K}$	$\log K_{Na,Rb}$	$\log K_{Na,Cs}$	$\log K_{Na,Ca}$	$\log K_{Na,Cu}$
Blank	−0.75	1.60	2.00	2.50	−1.65	−1.50
2	−0.25	0.80	1.15	1.55	−1.00	0.25
3	−0.30	0.70	1.05	1.60	−1.15	1.70
4	−0.25	0.75	1.05	1.50	−0.80	−0.75
11	−0.45	1.60	2.10	2.60	−1.35	−1.30

According to the results of our previous studies on sumanene molecular receptors,[22,26] PVC/2-nitrophenyl octyl ether (o-NPOE) membranes doped with receptors **2–4** exhibited high selectivity toward Cs$^+$. However, the specific structures of the bis- and tris-sumanenes **2–4** designed herein provided enhanced membrane selectivity toward Li$^+$ cations over other alkali metal cations, compared to the blank membranes (an increase in $\log K_{Na,Li}$ with a simultaneous decrease in $\log K_{Na,Me}$ values for other alkali metal cations[58]). Moreover, an enhanced affinity for Cu^{2+} cations was also noted, with the most pronounced effect observed for membranes based on receptor **3**, for which the highest selectivity for Cu^{2+} cations was obtained (higher even with respect to highly lipophilic Cs$^+$ cations).

This result was consistent with spectrofluorimetric titrations of the studied receptors, where a strong fluorescence quenching was registered for derivative **3** in the presence of Cu^{2+} cations. Despite the fact that potentiometric selectivity coefficients were determined in a heterogeneous system (membrane/water solution) and therefore did not strictly reflect the ion-binding properties of the studied receptors in solution, a satisfactory correlation of the electrochemical and spectroscopic results was noted.

As mentioned above, 1,2,3-triazole-based compounds are widely used as molecular receptors for selective recognition of Cu^{2+} cations.[33–35] Therefore, the selectivity of membranes doped with the truncated subunit of bis-sumanene **3**, namely 1,4-bis(1-benzyl-1H-1,2,3-triazol-4-yl)benzene (**11**; see the structure in Fig. 5),[59] was studied, to establish the role of 1,2,3-triazole sites in Cu^{2+} binding by receptor **3**. The incorporation of **11** into polymeric membranes led to a complete loss of their Cu^{2+} selectivity because a selectivity pattern similar to that obtained for blank membranes containing only the ion-exchanger was obtained. Such an effect was in satisfactory agreement with the results from our spectrofluorimetric experiment, where no significant change in the intensity of the fluorescence signal was observed during the titration of derivative **11** with copper cations (Fig. S39, SI).

These results clearly indicate that the affinity of receptor **3** for Cu^{2+} was not due to the interactions of the cations solely with the N-donor atoms of the 1,2,3-triazole moiety, but resulted from the complementary engagement of sumanene bowl(s) and 1,2,3-triazole binding sites in metal cation coordination (enhanced affinity for divalent metal was not observed for sumanene molecular receptors without the 1,2,3-triazole moiety, as reported in our previous work[22]).
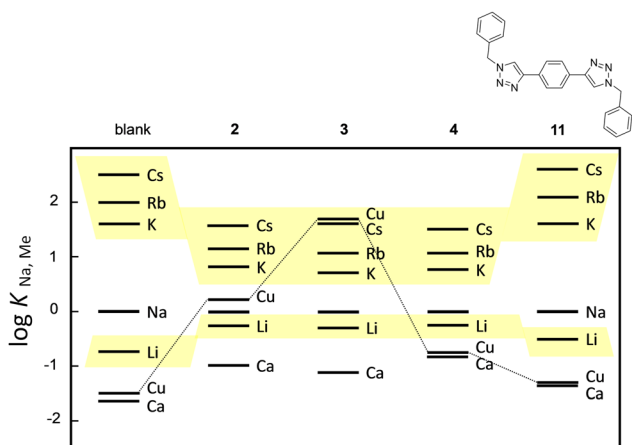
Fig. 5 Graphical presentation of the selectivity (values of $\log K_{Na,Me}$) of PVC/o-NPOE membranes formulated with receptors **2–4** and **11** (10 mol% KTFPB) and without a receptor (blank membrane); the mean values were calculated for 3 electrode specimens. The structure of compound **11** is also presented.

Our experimental results indicated that the presence of multiple sumanene units linked *via* 1,2,3-triazole skeletons strengthened the receptor affinity for Li$^+$ over other alkali metal cations. Moreover, the different cation selectivity of receptors **2–4** resulted from the specific location of the 1,2,3-triazole unit in the receptor structure (directly attached to the sumanene skeleton or *via* a linker). This unique arrangement of the binding sites in **3** was necessary to achieve high Cu^{2+} selectivity, whereas various geometrical features of the core skeleton in the structure of **3** (1,4-phenylene) in comparison to **4** (1,3,5-triphenyl-benzene) might have influenced the observed selectivity.

According to potentiometric and spectrofluorimetric studies with reference molecule **11**, the presence of the sumanene skeleton, providing cation–π interaction phenomenon in the designed molecules, was essential to tune their selectivity profiles. It also indicates that the binding mode for the studied receptors is related to the existence of cation–π interactions, in conjunction with N-oriented interactions with the included 1,2,3-triazole units.

To also study the role of sumanene bowls and 1,2,3-triazole binding sites in metal cation coordination, DFT calculations (B3LYP/3-21G) were conducted for the Li$^+$ complexes of receptor **2**, which exhibited the highest affinity for Li$^+$ cations among the studied receptors. Three different complex arrangements were subjected to DFT calculations, including the Li$^+$ cation, bound in a concave or convex site to the bowl-shaped parts of the receptor and assuming a 1:1 complex stoichiometry (see Table 3, where the free energies (ΔG) of complex formation and DFT-optimized structures are presented).

According to our computations, the most energetically favoured was the binding of Li$^+$ at the concave-oriented system, including the engagement of the 1,2,3-triazole moiety (arrangement **2_A**). It revealed a complementarity factor of sumanene and 1,2,3-triazole binding sites in the structure of receptor **2** for metal cation binding. However, the ΔG values for complex formation for convex-bound (arrangement **2_B**) and concave-bound Li$^+$ cation but with the 1,2,3-triazole moiety separated from the bowl by a phenyl ring (arrangement **2_C**) were significantly higher; ΔG for arrangement **2_B** was approximately twice as high as for **2_A**, whereas ΔG for arrangement

2_C was positive, suggesting the thermodynamically unfavoured formation of such a complex.

Notably, the obtained results also justify the lower values of the Stern–Volmer constants determined for derivatives **3** and **4**, in which the complementary engagement of a sumanene bowl and 1,2,3-triazole in metal cation coordination could not occur. It should be stressed that the above-noted experimental results from both techniques (spectrofluorimetry, potentiometry) are in satisfactory agreement and support highly specific **2**–Li$^+$ binding over other studied systems. In this sense, the DFT computations enabled insight to be obtained regarding the preferential binding mode of the studied system and revealed the crucial role of the presence of a 1,2,3-triazole moiety directly attached to a sumanene skeleton (*via* aromatic position), which improved cation–π interactions in the system. Such insight into Li$^+$ selectivity for sumanene-based receptors has not been previously reported.

The coordination chemistry of sumanene-based derivatives has been studied in recent years by many groups involved in the synthesis of these compounds. Depending on their structure, the complexation of various transition metal cations with a preference for metal binding to a concave surface *versus* a convex one has been reported.[4] Nevertheless, the receptor properties, especially the selectivity and sensitivity of the recognition of target molecules, were determined only for a limited number of sumanene derivatives dedicated for spectroscopic or electrochemical analyte sensing (see Table 4).

According to the first published computational and experimental studies, high affinity of sumanene receptors for caesium cations was observed. However, functionalisation of the sumanene bowl with a large terpyridine-ruthenium(II) moiety or the design of an aggregation-induced emission active (AIE) sumanene-1,1,2,2-tetraphenylethene derivative favored the complexation of lithium cations, predominantly at the convex side, according to the results of reported DFT computations. The results reported in our work demonstrate an important advancement in the design of a new generation of sumanene-based molecular receptors. Careful tuning of their structure may provide enhanced capabilities to sense lithium, copper, or caesium cations, as well as satisfactory binding parameters.

The results reported in this work demonstrate an important advancement in the design of new methods for the generation of sumanene-based molecular receptors, as careful tuning of their structure may provide enhanced sensing capabilities for lithium, copper, or caesium cations, with satisfactory binding parameters. Although this research aimed to synthesize and determine the coordination properties of new bis- and tris-sumanene derivatives, the electrochemical experiments carried out in a heterogeneous system emphasized their relevance in the development of modern electroanalytical tools.

Polymeric membranes are the key element of potentiometric sensors, whose high selectivity results from the recognition abilities of the appropriate molecular receptors, enabling their application for the monitoring of complex environmental samples. Therefore, the possibility of adapting the receptor structure based on the same sumanene motif, and thus the

Table 3 DFT-computed (B3LYP/3-21G) interaction energies (ΔG) and DFT-optimized (B3LYP/3-21G) structures of complexes formed from receptor **2** and Li$^+$ cations (hydrogen atoms are omitted for clarity)

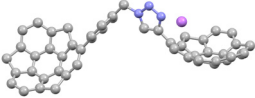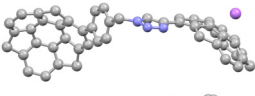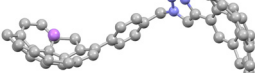| Arrangement	Geometry	ΔG [kJ mol^{-1}]
2_A		−112.7
2_B		−58.5
2_C		76.6

Table 4 Comparison of sensing performance for reported sumanene-based receptors

Receptor	Selectivity	Physicochemical parameter (M^{-1})	Analytical technique(s)	Ref.
Bis-sumanene (compound 2)	**Li$^+$**	**K_{SV}: 1.26×10^7**	**Fluorimetry, potentiometry**	**This work**
Tris-sumanene (compound 3)	**Cu^{2+}/Li$^+$**	**K_{SV}: from 1.0×10^6 to 2.6×10^6**		
Tris-sumanene (compound 4)	**Cs$^+$/Li$^+$**	**K_{SV}: from 3.87×10^6 to 2.48×10^6**		
Trisubstituted sumanenes (benzyl position)	Cs$^+$	K_a: from 2.88×10^4 to 7.35×10^6	fluorimetry, potentiometry, voltammetry (ferrocene derivatives)	12, 22 and 24–27
Monosubstituted sumanenes (aromatic position)	Cs$^+$	K_{SV}: from 1.70×10^4 to 4.50×10^5 K_a: from 5.90×10^5 to 8.70×10^5	fluorimetry, potentiometry, voltammetry (ferrocene derivatives)	11, 22 and 40
Tetrasubstituted sumanenes (both benzyl and aroamtic positions)	Cs$^+$	K_a: from 3.90×10^3 to 1.20×10^5	fluorimetry, voltammetry (ferrocene derivatives)	27 and 28
Sumanenes featuring an aggregation-induced emission effect (aromatic or benzylic position)	Cs$^+$/Li$^+$	K_{SV}: from 4.54×10^8 to 4.68×10^{10}	fluorimetry	23
Sumanene-based terpyridine-ruthenium(II) complexes (aromatic position)	Li$^+$	K_{SV}: from 0.73×10^3 to 5.05×10^3	fluorimetry	39

selectivity and sensitivity of a designed sensor to a specific analytical task, is particularly important.

Conclusions

Our work demonstrates the possibility for the synthesis of bis- and tris-sumanene derivatives using the *click chemistry* approach. The obtained molecules were applied to the optical and potentiometric detection of metal cations, which revealed the structure–receptor property relationship of the designed sumanene-based receptors. Depending on the receptor structure, specifically the type and geometrical features of the linker between the sumanene skeletons, as well as the mode of attachment of a 1,2,3-triazole unit to a sumanene core, different recognition properties toward Cs$^+$, Li$^+$, or Cu^{2+} cations were observed.

Notably, the results from spectrofluorimetric titrations and potentiometric experiments were in satisfactory accordance and were further supported by DFT computations for the representative system. We believe this work opens new pathways for designing sumanene-based organic materials with tuned receptor properties for detecting metal cations, ranging from small Li$^+$ cations to large Cs$^+$ cations, as well as d-block Cu^{2+} cations.

Author contributions

J. A. performed synthesis, characterization, receptor (potentiometric, spectroscopic) experiments and DFT computations under the supervision of A. K. and W. W., analysed the data, prepared the manuscript text dealing with spectrofluorimetric titrations and DFT computations, as well as compiled SI regarding these parts. S. K. performed the calculations for the Stern–Volmer constants, prepared the text regarding this part of the work, and commented on the manuscript during the preparation of the final version. H. S. provided sumanene, funding for research from the Japanese side, and commented on the manuscript during the preparation of the final version. W. W. co-conceived the project, designed and supervised

potentiometric and spectrofluorimetric experiments performed by J. A., analysed the data, prepared a draft of the manuscript text on the potentiometric studies, as well as compiled SI regarding this part, wrote part of the introduction section, and co-conceptualized and commented on the manuscript during the preparation of the final version. A. K. conceived the project, designed the structures of all compounds, designed and supervised the synthetic, spectrofluorimetric, and DFT computational experiments performed by J. A., performed and compiled the results of TD-DFT computations, analysed the data, prepared a draft of the synthesis and characterization sections in the manuscript, compiled the manuscript and SI, wrote most parts of the introduction section, co-conceptualized and commented on the manuscript during the preparation of the final version, provided funding for research from the Polish side, and corresponded with the Editor and Reviewers.

Conflicts of interest

There are no conflicts to declare. All authors have approved the final version of the manuscript.

Data availability

The data supporting this article have been included as part of the SI.

Materials and methods, experimental procedures, compounds characterization data, additional data on receptor studies, DFT computational details. See DOI: **https://doi.org/10.1039/d5tc02182k**

Acknowledgements

Notes and references

1 H. Sakurai, T. Daiko and T. Hirao, *Science*, 2003, **301**, 1878.

2 A. Kasprzak, *Angew. Chem., Int. Ed.*, 2024, **63**, e202318437.

3 M. Saito, H. Shinokubo and H. Sakurai, *Mater. Chem. Front.*, 2018, **2**, 635.

4 T. Amaya and T. Hirao, *Chem. Rec.*, 2015, **15**, 310.

5 T. Amaya and T. Hirao, *Chem. Commun.*, 2011, **47**, 10524.

6 M. Li, J. Wu, K. Sambe, Y. Yakiyama, T. Akutagawa, T. Kajitani, T. Fukushima, K. Matsuda and H. Sakurai, *Mater. Chem. Front.*, 2022, **6**, 1752.

7 Y. Yakiyama, M. Li and H. Sakurai, *Pure Appl. Chem.*, 2023, **95**, 421.

8 Y. Yakiyama, M. Li, D. Zhou, T. Abe, C. Sato, K. Sambe, T. Akutagawa, T. Matsumura, N. Matubayasi and H. Sakurai, *J. Am. Chem. Soc.*, 2024, **146**, 5224.

9 I. Hisaki, H. Toda, H. Sato, N. Tohnai and H. Sakurai, *Angew. Chem., Int. Ed.*, 2017, **56**, 15294.

10 Y. Yakiyama, T. Hasegawa and H. Sakurai, *J. Am. Chem. Soc.*, 2019, **141**, 18099.

11 A. Kasprzak and H. Sakurai, *Dalton Trans.*, 2019, **48**, 17147.

12 A. Kasprzak, A. Kowalczyk, A. Jagielska, B. Wagner, A. M. Nowicka and H. Sakurai, *Dalton Trans.*, 2020, **49**, 9965.

13 A. Kasprzak, A. Gajda-Walczak, A. Kowalczyk, B. Wagner, A. M. Nowicka, M. Nishimoto, M. Koszytkowska-Stawińska and H. Sakurai, *J. Org. Chem.*, 2023, **88**, 4199.

14 D. Vijay, H. Sakurai, V. Subramanian and G. N. Sastry, *Phys. Chem. Chem. Phys.*, 2012, **14**, 3057.

15 J. A. Carrazana-García, E. M. Cabaleiro-Lago and J. Rodríguez-Otero, *Phys. Chem. Chem. Phys.*, 2017, **19**, 10543.

16 A. Campo-Cacharrón, E. M. Cabaleiro-Lago and J. Rodríguez-Otero, *J. Comput. Chem.*, 2014, **35**, 1533.

17 U. D. Priyakumar and G. N. Sastry, *Tetrahedron Lett.*, 2003, **44**, 6043.

18 S. N. Spisak, Z. Wei, A. Yu. Rogachev, T. Amaya, T. Hirao and M. A. Petrukhina, *Angew. Chem., Int. Ed.*, 2017, **56**, 2582.

19 T. Amaya, H. Sakane and T. Hirao, *Angew. Chem.*, 2007, **119**, 8528.

20 T. Amaya and T. Hirao, in *Advances in Organometallic Chemistry and Catalysis*, ed. A. J. L. Pombeiro, John Wiley & Sons, Inc., Hoboken, NJ, USA, 2013, pp. 473–483.

21 S. N. Spisak, Z. Wei, N. J. O'Neil, A. Yu. Rogachev, T. Amaya, T. Hirao and M. A. Petrukhina, *J. Am. Chem. Soc.*, 2015, **137**, 9768.

22 J. Ażgin, M. Wesoły, K. Durka, H. Sakurai, W. Wróblewski and A. Kasprzak, *Dalton Trans.*, 2024, **53**, 2964.

23 J. S. Cyniak, H. Sakurai and A. Kasprzak, *Chem. – Eur. J.*, 2025, **31**, e202500705.

24 J. S. Cyniak, Ł. Kocobolska, N. Bojdecka, A. Gajda-Walczak, A. Kowalczyk, B. Wagner, A. M. Nowicka, H. Sakurai and A. Kasprzak, *Dalton Trans.*, 2023, **52**, 3137.

25 A. Kasprzak and H. Sakurai, *Chem. Commun.*, 2021, **57**, 343.

26 A. Kasprzak, A. Tobolska, H. Sakurai and W. Wróblewski, *Dalton Trans.*, 2022, **51**, 468.

27 D. Ufnal, J. S. Cyniak, M. Krzyzanowski, K. Durka, H. Sakurai and A. Kasprzak, *Org. Biomol. Chem.*, 2024, **22**, 5117.

28 A. Kasprzak, A. Zuchowska, P. Romanczuk, A. Kowalczyk, I. P. Grrudziński, A. Malkowska, A. M. Nowicka and H. Sakurai, *Dalton Trans.*, 2024, **53**, 56.

29 J. E. Moses and A. D. Moorhouse, *Chem. Soc. Rev.*, 2007, **36**, 1249.

30 H. M. Pineda-Castañeda, Z. J. Rivera-Monroy and M. Maldonado, *ACS Omega*, 2023, **8**, 3650.

31 M. Juríček, P. H. J. Kouwer and A. E. Rowan, *Chem. Commun.*, 2011, **47**, 8740.

32 Y. Hua and A. H. Flood, *Chem. Soc. Rev.*, 2010, **39**, 1262.

33 J. Košmrlj, *Click Triazoles*, Springer Berlin Heidelberg, Berlin, Heidelberg, 2012, vol. 28.

34 U. Salma, Md. Z. Alam, S. Ahmad, Md Mohasin and S. A. Khan, *Inorg. Chim. Acta*, 2025, 122600.

35 J. B. Czirok, G. Jágerszki, K. Tóth, Á. Révész, L. Drahos and I. Bitter, *J. Inclusion Phenom. Macrocyclic Chem.*, 2014, **78**, 207.

36 E. M. Zahran, Y. Hua, Y. Li, A. H. Flood and L. G. Bachas, *Anal. Chem.*, 2010, **82**, 368.

37 J. Camponovo, J. Ruiz, E. Cloutet and D. Astruc, *Chem. – Eur. J.*, 2009, **15**, 2990.

38 S. Kaur Shalini, B. Ahmad Shiekh, V. Kumar and I. Kaur, *J. Electroanal. Chem.*, 2022, **905**, 115966.

39 J. Han, Y. Yakiyama, Y. Takeda and H. Sakurai, *Inorg. Chem. Front.*, 2023, **10**, 211.

40 A. Kasprzak, A. Gajda-Walczak, A. Kowalczyk, B. Wagner, A. M. Nowicka, M. Nishimoto, M. Koszytkowska-Stawińska and H. Sakurai, *J. Org. Chem.*, 2023, **88**, 4199.

41 J. Wang, D. Liang, J. Feng and X. Tang, *Anal. Chem.*, 2019, **91**, 11045.

42 P. Li, X. Wang, S. Y. Tan, C. Y. Ang, H. Chen, J. Liu, R. Zou and Y. Zhao, *Angew. Chem., Int. Ed.*, 2015, **54**, 12748.

43 S. Viel, F. Ziarelli, G. Pagès, C. Carrara and S. Caldarelli, *J. Magn. Reson.*, 2008, **190**, 113.

44 E. Aprà, E. J. Bylaska, W. A. De Jong, N. Govind, K. Kowalski, T. P. Straatsma, M. Valiev, H. J. J. Van Dam, Y. Alexeev, J. Anchell, V. Anisimov, F. W. Aquino, R. Atta-Fynn, J. Autschbach, N. P. Bauman, J. C. Becca, D. E. Bernholdt, K. Bhaskaran-Nair, S. Bogatko, P. Borowski, J. Boschen, J. Brabec, A. Brunauer, E. Cauët, Y. Chen, G. N. Chuev, C. J. Cramer, J. Daily, M. J. O. Deegan, T. H. Dunning, M. Dupuis, K. G. Dyall, G. I. Fann, S. A. Fischer, A. Fonari, H. Früchtl, L. Gagliardi, J. Garza, N. Gawande, S. Ghosh, K. Glaesemann, A. W. Götz, J. Hammond, V. Helms, E. D. Hermes, K. Hirao, S. Hirata, M. Jacquelin, L. Jensen, B. G. Johnson, H. Jónsson, R. A. Kendall, M. Klemm, R. Kobayashi, V. Konkov, S. Krishnamoorthy, M. Krishnan, Z. Lin, R. D. Lins, R. J. Littlefield, A. J. Logsdail, K. Lopata, W. Ma, A. V. Marenich, J. Martin Del Campo, D. Mejia-Rodriguez, J. E. Moore, J. M. Mullin, T. Nakajima, D. R. Nascimento, J. A. Nichols, P. J. Nichols, J. Nieplocha, A. Otero-de-la-Roza, B. Palmer, A. Panyala, T. Pirojsirikul,

B. Peng, R. Peverati, J. Pittner, L. Pollack, R. M. Richard, P. Sadayappan, G. C. Schatz, W. A. Shelton, D. W. Silverstein, D. M. A. Smith, T. A. Soares, D. Song, M. Swart, H. L. Taylor, G. S. Thomas, V. Tipparaju, D. G. Truhlar, K. Tsemekhman, T. Van Voorhis, Á. Vázquez-Mayagoitia, P. Verma, O. Villa, A. Vishnu, K. D. Vogiatzis, D. Wang, J. H. Weare, M. J. Williamson, T. L. Windus, K. Woliński, A. T. Wong, Q. Wu, C. Yang, Q. Yu, M. Zacharias, Z. Zhang, Y. Zhao and R. J. Harrison, *J. Chem. Phys.*, 2020, **152**, 184102.

45 M. J. Frisch, G. W. Trucks, H. B. Schlegel, G. E. Scuseria, M. A. Robb, J. R. Cheeseman, G. Scalmani, V. Barone, G. A. Petersson, H. Nakatsuji, X. Li, M. Caricato, A. V. Marenich, J. Bloino, B. G. Janesko, R. Gomperts, B. Mennucci, H. P. Hratchian, J. V. Ortiz, A. F. Izmaylov, L. Sonnenberg, D. Williams-Young, F. Ding, F. Lipparini, F. Egidi, J. Goings, B. Peng, A. Petrone, T. Henderson, D. Ranasinghe, V. G. Zakrzewski, J. Gao, N. Rega, G. Zheng, W. Liang, M. Hada, M. Ehara, K. Toyota, R. Fukuda, J. Hasegawa, M. Ishida, T. Nakajima, Y. Honda, O. Kitao, H. Nakai, T. Vreven, K. Throssell, J. A. MontgomeryJr, J. E. Peralta, F. Ogliaro, M. J. Bearpark, J. J. Heyd, E. N. Brothers, K. N. Kudin, V. N. Staroverov, T. A. Keith, R. Kobayashi, J. Normand, K. Raghavachari, A. P. Rendell, J. C. Burant, S. S. Iyengar, J. Tomasi, M. Cossi, J. M. Millam, M. Klene, C. Adamo, R. Cammi, J. W. Ochterski, R. L. Martin, K. Morokuma, O. Farkas, J. B. Foresman and D. J. Fox, *Gaussian 16, Revision C.01*, Gaussian, Inc., Wallingford CT, 2016.

46 R. Dennington, T. A. Keith and J. M. Millam, *GaussView, Version 6.1*, Semichem Inc., Shawnee Mission, KS, 2016.

47 M. D. Hanwell, D. E. Curtis, D. C. Lonie, T. Vandermeersch, E. Zurek and G. R. Hutchison, *J. Cheminf.*, 2012, **4**, 17.

48 Avogadro: An Open-Source Molecular Builder and Visualization Tool. Version 1.2.0. **https://Http://Avogadro.cc/.**

49 A. D. Becke, *J. Chem. Phys.*, 1993, **98**, 5648.

50 J. S. Binkley, J. A. Pople and W. J. Hehre, *J. Am. Chem. Soc.*, 1980, **102**, 939.

51 M. Bardhan, G. Mandal and T. Ganguly, *J. Chem. Phys.*, 2009, **106**, 034701.

52 P. Basak, T. Debnath, R. Banerjee and M. Bhattacharyya, *Front. Biol.*, 2016, **11**, 32.

53 B. U. Rajapakshe, Y. Li, B. Corbin, K. J. Wijesinghe, Y. Pang and C. S. Abeywickrama, *Chemosensors*, 2022, **10**, 382.

54 E. Bakker, P. Bühlmann and E. Pretsch, *Chem. Rev.*, 1997, **97**, 3083.

55 P. Bühlmann, E. Pretsch and E. Bakker, *Chem. Rev.*, 1998, **98**, 1593.

56 P. C. Meier, W. E. Morf, M. Läubli and W. Simon, *Anal. Chim. Acta*, 1984, **156**, 1–8.

57 Y. Marcus, *J. Chem. Soc., Faraday Trans.*, 1991, **87**, 2995.

58 More pronounced increase of the membrane ion-selectivity towards lithium against caesium cations is visible in Figure located in Section S5 (SI), presenting the values of selectivity coefficients calculated for Cs^+ as the primary ion.

59 S. Ø. Scott, E. L. Gavey, S. J. Lind, K. C. Gordon and J. D. Crowley, *Dalton Trans.*, 2011, **40**, 12117.